1.0 THz f_{max} InP DHBTs in a refractory emitter and self-aligned base process for reduced base access resistance

Vibhor Jain[1], Johann C. Rode[1], Han-Wei Chiang[1], Ashish Baraskar[1], Evan Lobisser[1], Brian J. Thibeault[1], Mark Rodwell[1], Miguel Urteaga[2], D. Loubychev[3], A. Snyder[3], Y. Wu[3], J. M. Fastenau[3], W.K. Liu[3]

[1]ECE Department, University of California, Santa Barbara, CA 93106-9560
Phone: 805-893-3273, Fax: 805-893-3262, Email: vibhor@ece.ucsb.edu
[2]Teledyne Scientific & Imaging, Thousand Oaks, CA 91360
[3]IQE Inc., 119 Technology Drive, Bethlehem, PA 18015

We report 220 nm InP double heterojunction bipolar transistors (DHBTs) demonstrating f_τ = 480 GHz and f_{max} = 1.0 THz. Improvements in the emitter and base processes have made it possible to achieve a 1.0 THz f_{max} even at 220 nm wide emitter-base junction with a 1.1 μm wide base-collector mesa. A vertical emitter metal etch profile, wet-etched thin InP emitter semiconductor with less than 10 nm undercut and self-aligned base contact deposition reduces the emitter semiconductor-base metal gap (W_{gap}) to ~ 10 nm, thereby significantly reducing the gap resistance term (R_{gap}) in the total base access resistance (R_{bb}), enabling a high f_{max} device. Reduction in the total collector base capacitance (C_{cb}) through undercut in the base mesa below base post further improved f_{max}. These devices employ a Mo/W/TiW refractory emitter metal contact which allows biasing the transistors at high emitter current densities (J_e) without problems of electromigration or contact diffusion under electrical stress [1].

Improved bandwidth for the HBTs can be achieved through epitaxial scaling of base (T_b) and collector (T_c) thicknesses for reduced transit delays; and lithographic scaling with lower contact resistivities for reduced RC delays [2]. For the DHBTs reported here, emitter design includes a 10 nm thick highly doped n-$In_{0.53}Ga_{0.47}As$ cap ($N_d > 5 \times 10^{19}$ cm^{-3}) for reduced contact resistivity and a thin (30 nm) InP layer for controlled emitter undercut and reduced emitter depletion region resistance [3]. InGaAs base is 30 nm thick having a $9 - 5 \times 10^{19}$ cm^{-3} doping gradient and T_c is 100 nm. The base-collector grade includes a 13.5 nm InGaAs setback and a 16.5 nm InGaAs/InAlAs chirped-superlattice grade. The epitaxial structure was grown by IQE Inc. on a 4" semi-insulating InP substrate [4]. Extrinsic base, in the emitter-base gap (W_{gap}), has a higher sheet resistance ($R_{sh,ex}$) than intrinsic base due to surface depletion from Fermi level pinning and surface damage from processing – $R_{sh,ex}$ = 920 Ω/sq and $R_{sh,int}$ = 710 Ω/sq measured from pinched and non-pinched TLM measurements. Thus, $R_{gap} = R_{sh,ex} \cdot W_{gap} / 2 \cdot L_e$ becomes a dominant component of R_{bb} for large W_{gap} [2]. For these HBTs, dry etch for Mo/W/TiW (10% Ti by weight) stack is optimized to obtain a vertical emitter metal profile; thin (30 nm) InP emitter layer is wet-etched for controlled semiconductor undercut (< 10 nm) and self-aligned base contact (Pt/Ti/Pd/Au) lift-off process is used. These features greatly reduce W_{gap}, and therefore R_{gap}, consequently increasing f_{max}. This reduction in R_{bb} made it possible to achieve 1.0 THz f_{max} even at 220 nm wide emitter with a 1.1 μm wide, misaligned base mesa. Fabrication details are as in [4].

1-67 GHz measurements of HBTs embedded in a ground-signal-ground pad structure were carried out after performing a standard line-reflect-reflect-match (LRRM) calibration on an Agilent E8361A PNA, bringing the reference planes to the probe tips. On wafer, short and open circuit pad structures identical to those used by the devices were measured after calibration to de-embed associated transistor pad parasitics. The same calibration and de-embedding procedures were used for 80-105 GHz measurements on Agilent 8510XF system. Peak RF performance for HBTs with A_{je} = 0.22 × 2.7 μm^2 was obtained at I_c = 12.1 mA and V_{ce} = 1.64 V (V_{cb} = 0.7 V, J_e = 20.4 mA/μm^2, P = 33.4 mW/μm^2). Extrapolations from single-pole fit to the measured current gain H_{21} and Mason's Unilateral gain U indicate cut off frequencies f_τ = 480 GHz and f_{max} = 1.0 THz. Total emitter access resistivity ρ_{ex} ~ 4.2 Ω-μm^2 was extracted from RF data. HBTs with an emitter junction width of 220 nm (W_e) show peak DC common emitter current gain β = 17 and common emitter breakdown voltage $V_{BR,CEO}$ = 3.7 V (J_e = 0.1 mA/um^2). The Kirk effect is observed at J_e = 23 mA/μm^2 (V_{cb} = 0.7 V) when f_τ falls to 95% of its peak value.

A linear fit to the extracted C_{cb} variation with emitter length (L_e) has ~ 0 fF intercept suggesting negligible capacitance contribution from the base post. This is also evident from weak dependence of f_τ on L_e; peak f_τ changes from 480 GHz to 465 GHz for L_e increase from 3 μm to 5 μm. For low R_{bb}, base metal resistance $R_{metal} = R_{sh,m} \cdot L_e / 6 \cdot W_{bc}$ [2] becomes a significant fraction of total R_{bb} and thus f_{max} decreases with increase in L_e. Further improvement in f_τ/f_{max} can be achieved through reduced emitter and base-collector junction areas and lower contact resistivities.

This work was supported by the DARPA THETA program under HR0011-09-C-0060. A portion of this work was done in the UCSB nanofabrication facility, part of NSF funded NNIN network and MRL Central Facilities supported by the MRSEC Program of the NSF under award No. MR05-20415

[1] Y. K. Fukai *et al.*, *Microelectronics Reliability*, vol. 49, no. 4, pp. 357-364, April 2009
[2] M. J. W. Rodwell *et al.*, *Proc. of the IEEE*, vol. 96, no. 2, pp. 271-286, Feb 2008
[3] V. Jain *et al.*, *Electron Device Letters, IEEE*, vol. 32, no.1, pp.24-26, Jan 2011
[4] V. Jain *et al.*, to be presented at *International Conference on Indium Phosphide and Related Materials (IPRM)*, May 2011

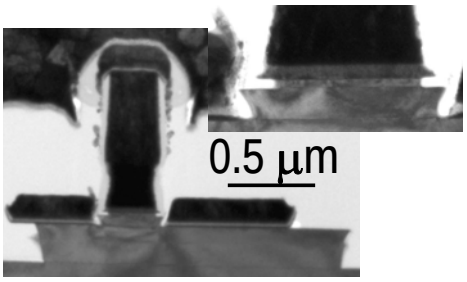

Fig. 1. Cross-sectional TEM of emitter mesa of DHBT showing the emitter profile with 220 nm wide emitter-base junction and 1.1 µm wide, non-symmetric base-collector mesa. Magnified view of the emitter mesa shows the small undercut in InP emitter and narrow base-emitter gap (W_{gap} ~10 nm)

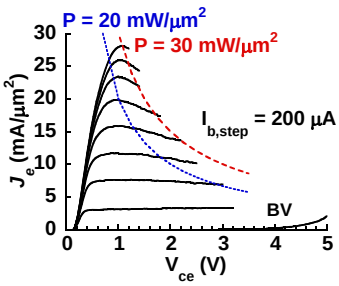

Fig. 2. Common-Emitter current density-voltage (J_e-V) characteristics of a DHBT with A_{je} = 0.22 × 4.7 µm²

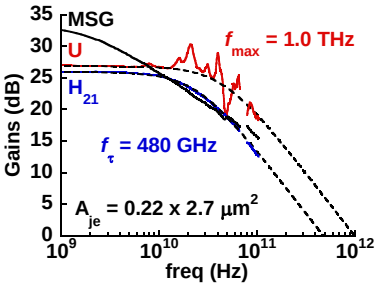

Fig. 3. Measured RF gains for the DHBT in 1 - 67 GHz and 80-105 GHz bands using off-wafer LRRM calibration in a lumped pad structure. The DHBT was biased at I_c = 12.1 mA, V_{ce} = 1.64 V

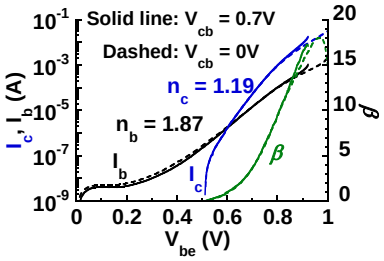

Fig. 4. Gummel Plot of a DHBT with A_{je} = 0.22 × 4.7 µm²

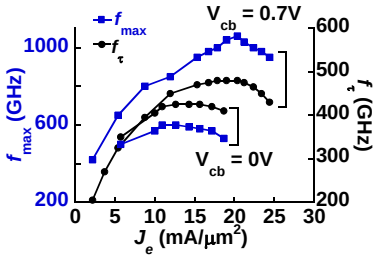

Fig 5. f_τ/f_{max} dependence on V_{cb} and J_e

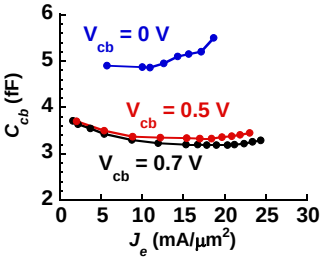

Fig 6. Variation in C_{cb} with V_{cb} and J_e

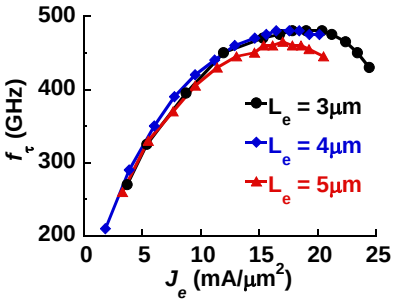

Fig 7. Variation in f_τ with J_e for different L_e at V_{cb} = 0.7 V for DHBTs having W_e = 220 nm and same base-collector mesa width

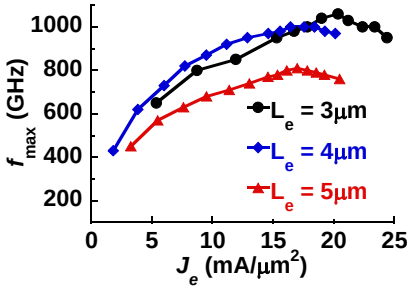

Fig 8. Variation in f_{max} with J_e for different L_e at V_{cb} = 0.7 V for DHBTs having W_e = 220 nm and same base-collector mesa width

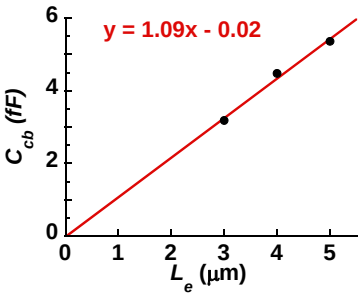

Fig 9. Variation in extracted C_{cb} with L_e for W_e = 220 nm and same base-collector mesa width

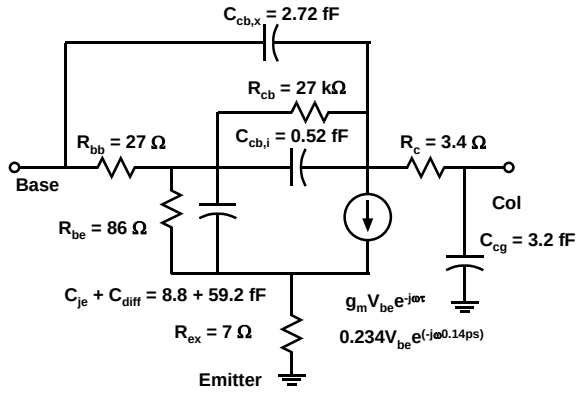

Fig 10. Hybrid-π equivalent circuit at peak RF performance from 1 – 67 GHz RF data for the bias conditions: I_c = 12.1 mA, V_{ce} = 1.64 V

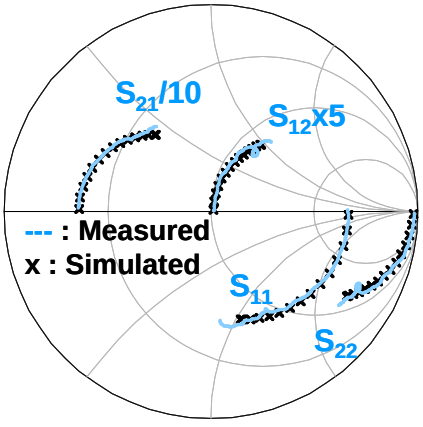

Fig 11. 1 - 67 GHz measured and simulated S-Parameters from equivalent circuit model in Fig 10